Microcontroller Based Implementation of Fuel Cell and Battery Integrated Hybrid Power Source

[1]Fahad Ali, [2]Syed Mohsin Ali, [3]Dr. Abdul Aziz Bhatti, [4]Mashood Nasir

[1]fahad.ali@umt.edu.pk [2]syed.mohsin@umt.edu.pk [3]drabhatti@umt.edu.pk [4]mashood.nasir@umt.edu.pk

University of Management & Technology Lahore, Pakistan

Abstract— *This paper presents the implementation of a digitally controlled hybrid power source system, composed of fuel cell and battery. Use of individual fuel cell stacks as a power source, encounters many problems in achieving the desired load characteristics. A battery integrated, digitally controlled hybrid system is proposed for high pulse requirements. The proposed hybrid power source fulfils these peak demands with efficient flow of energy as compared to individual operations of fuel cell or battery system. A dc/dc converter is applied which provides an optimal control of power flow among fuel cell, battery and load. The proposed system efficiently overcomes the electrochemical constraints like over current, battery leakage current, and over and under voltage dips. By formulation of an intelligent algorithm and incorporating a digital technology (AVR Microcontroller), an efficient control is achieved over fuel cell current limit, battery charge, voltage and current. The hybrid power source is tested and analyzed by carrying out simulations using MATLAB simulink. Along with the attainment of desired complex load profiles, the proposed design can also be used for power enhancement and optimization for different capacities.*

Keywords- Fuel cell, Hybrid Power Source, Energy Storage Management

I. INTRODUCTION (HEADING 1)

Now a day's fuel cells are showing enormous potential for several areas of applications [4-8]. However, many applications have a common characteristic in their load profiles, that is, they have a relatively low average power demand but a relatively high pulse power requirement. The pulse duration in these applications generally ranges from hundreds of milliseconds to minutes, depending upon the power level of the applications. The hybrid power sources composed of Fuel cell/battery can fulfill these pulse power requirements with higher specific power and efficiency than the fuel cell or battery alone while still preserving high energy density [8-14]. The passive hybrid source, results from connecting both the fuel cell and the battery directly to the power bus [8]. The output power capacity in the active hybrid source is greater than the passive hybrid source, as illustrated in Fig. 1. Due to these limitations of the passive hybrid, a dc/dc power converter is placed between the fuel cell and the battery so that they may have different voltage levels [9-14].

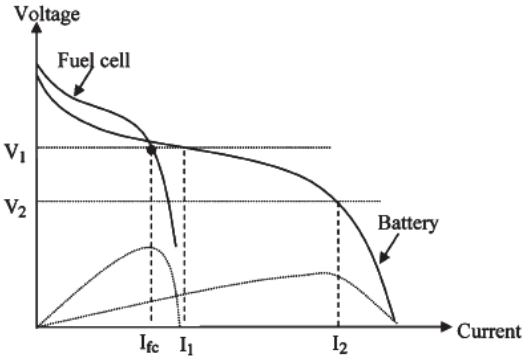

Fig. 1. Voltage-Current (V-I) curves of the fuel cell and the battery

Where;
V_1: Fuel Cell voltage at max. Power
V_2: Battery voltage in the active
I_{fc}: Fuel Cell current at max. Power
I_1: Battery discharging current in the passive
I_2: Battery discharging current in the active

The power architecture and control scheme dedicated for hybrid fuel cell/battery sources must provide an uninterrupted power flow to the load. Power controllers for hybrid power sources used complicated analog circuits before [1]. Analog control provides continuous processing of the signal, hence allowing a high bandwidth, giving infinite resolution of the measured signal. Digital control is striking to modern power electronics controls due to many advantages over analog control such as programmability, user friendly, easy control, less susceptibility to environmental variations. Also digital control allows designers to easily implement very complex algorithmic controls and to amend the algorithm properly.

Though conventional digital controllers based on discrete logic components require complex peripheral and auxiliary circuits [2,3], an Alf-Egil Bogen, Vegard Wollan, RISC (AVR) microcontroller is used in this study to control the active hybrid power source.

This paper presents a compact digitally controlled fuel cell/battery hybrid power source based on a small number of parts. The architecture of the hybrid system and the implementation of the digital power controller are presented in Section II. In Section III, a control algorithm that is suitable for regulating multiple variables in the hybrid system is described by using a state machine model; the issues of embedded control implementation are addressed; and the

large-signal behavior of the hybrid system is analyzed. Simulation and experiment results are given and analyzed in Section IV.

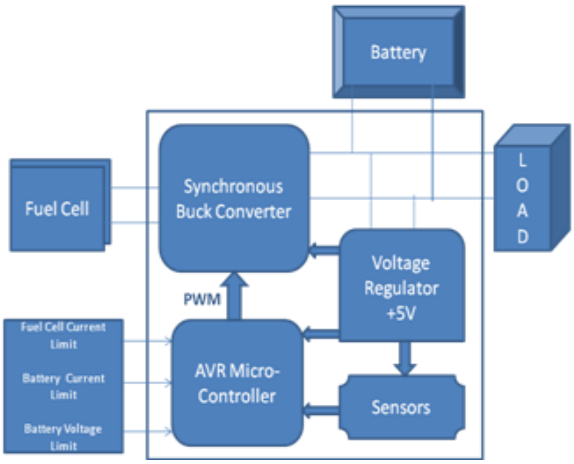

Fig. 2. Fuel Cell/Battery hybrid power source (Digital Controlling)

II. INTELLIGENT CONTROLLING OF HYBRID POWER SOURCES

A. Basic Architecture of Active Hybrid Power Sources

In this study, the hybrid power source consists of a proton exchange membrane (PEM) fuel cell stack with a nominal power of 1.26 kW, a Nickel-Metal-Hydride battery, and a digital power controller, as shown in Fig. 2.This digital power controller circuit comprises a synchronous buck converter that is controlled by an AVR microcontroller, current, voltage and temperature sensors, and a voltage regulator that powers these components. All mechanism and controlling of this Hybrid Power Source is maintained through the microcontroller software.

B. Power Controller

The architecture of digital power controller for fuel cell/battery hybrid power sources is shown in the fig. 3. As here illustrated, the load is directly connected to the battery, an H-bridge-based DC-DC buck converter is connected between the fuel cell and the load. Here the H-bridge is controlling the fundamental operation of the hybrid power source.The high power demands of load is satisfied by the battery which provides additional power and is charged by the fuel cell when the load is low. The R_SENSE_fc and R_SENSE_bat are the two current sensing resistors for the fuel cell and the battery respectively. Both of the resistors have values 0.1 Ω, and are amplified by the amplification factor of 10, so that the outputs of the current amplifier are the actual values of the currents measured. The voltage of the battery is measured by a voltage divider with a gain of 0.25 since the voltage range of the battery used in this study is from 10 to 18 V and the full dynamic range of the A/D converter is from 0 to 5 V. The AVR microcontroller (model ATmega16) is fed with the measured values of the fuel cell current, battery current, and battery voltage. The AVR (ATmega16) is high performance low power Advanced Risc Based 8 bit microcontroller, featuring of 16kb of In System self programmable flash, 512 bytes of internal EEPROM, six PWM channel for high speed operation with programmable resolution from 2 to 11bits, 12 channel 10 bit ADC and programmable serial USART. FCCL, BCL, and BVL are preset by the users. The duty cycles of dc-dc buck converter are controlled by the digital controller based on the measured signals and produces a continuous PWM signal from which the H-bridge is derived.

III. CONTROL SYSTEM

A. Strategy

As we discussed about the control software running on the microcontroller, the objective of this software is to generate an appropriate PWM switching signal for the dc/dc power converter. The output current of the fuel cell, the voltage, or the current of the battery can be regulated by changing duty cycle of the PWM switching signal. There are three regulation modes for control software for this system, namely:

1) FCCL mode
2) BCL mode
3) BVL mode

If the battery voltage exceeds the voltage limit, the BVL mode applies, which may correspond to the condition of no load or light load coupled with high battery charge,. Under this mode, the output current of the fuel cell and the charging current of the battery should be below the rated currents.

If the battery voltage is below the voltage limit, which may correspond to the condition of heavy load or light load coupled with low battery charge, the FCCL or BCL mode may apply depending on the load.

If the current demand is lower than the rated output current of the fuel cell, the charging current of the battery may need to be regulated in order to protect the battery, i.e., the BCL mode is applied. In this case, the fuel cell current is unregulated but is always below the rated current.

If the current demand is very high, the FCCL mode applies, and the fuel cell current is regulated at the limit (the rated current). In this case, the battery may be discharged or charged at a lower rate.

If the battery voltage drops below a preset low value (low voltage disconnecting point), the load will be disconnected from the power source to protect the battery from over discharging. All this phenomenon of the control software is shown in Fig. 5. The blocks represent the regulation modes and the arrows show the event-triggered transitions between modes.

These events happen under the corresponding conditions. For example, when the power source is first turned on, it works in FCCL mode. If there is no load or a light load, the charging current of the battery may increase fast from zero to its limit, and then the BCL mode applies. When the battery voltage

reaches the voltage limit, the BVL mode applies. Under either BCL or BVL mode, if the load increases very fast (i.e., when the fuel cell current reaches the limit), the FCCL mode will apply. At any moment, the control strategy selects only one regulation mode. When any change in the fuel cell, the battery, or the load results in the satisfaction of the corresponding event condition, the controller will operate at another regulation mode. In the system shown in Fig. 2, the control strategy takes into account all the regulation modes and the conditions that result in the change of regulation mode. Under any condition of the load, the control strategy can decide the regulation mode correctly, as shown later in this paper. Thus, the control strategy is able to regulate the fuel cell current, the charging current, or the voltage of the battery by using only one control variable.

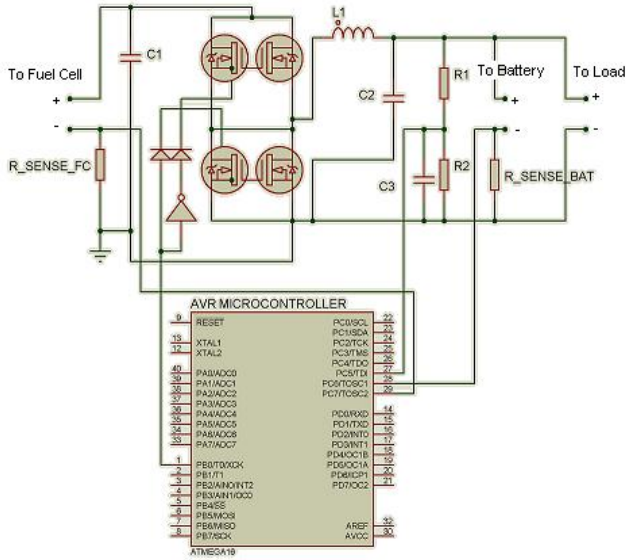

Fig. 4. Schematic Diagram of the proposed Digital power Controller for the hybrid power source

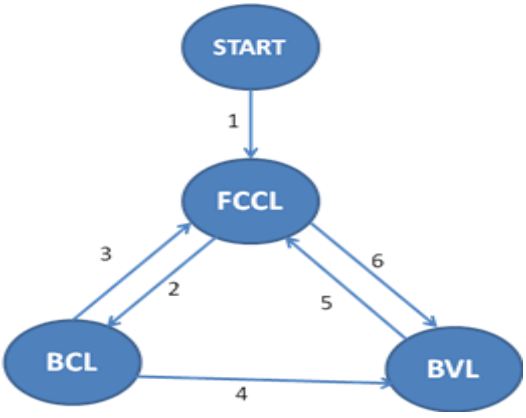

Fig. 5. Control Algorithm representation for the fuel cell/battery hybrid power source

B. Controlling

A modified proportional–integral (PI) approach is used to regulate the currents and voltage. The controller has different compensation objectives when different regulation modes are selected. In order to reduce the voltage or current transients that may occur when the regulation mode is changed, the control scheme consists of a feed forward term (implemented by the duty cycle at the previous sample interval) plus the proportional and integral terms of the errors of the currents or voltage. The duty cycle at the previous sample interval was stored in memory for calculation of the duty cycle at the present step. The proportional and integral terms of the errors are actually compensating the change of the duty cycle ($\Delta\partial$) at the present step. By doing this, the duty cycle will not change a lot at the time of mode change, and both the fuel cell current and the battery current can be regulated within the limits, even if transitions 2 and 3 may potentially be oscillatory when Ibat_REF and Ifc_REF are not selected appropriately or if the load varies frequently, because the effect of the fuel cell current error on the change of the duty cycle is similar to that of the battery charging current error. Whenever the regulation mode is changed, each integrator is reset to avoid unusual current or voltage transients at the time of mode change. The current and voltage regulations are formulated as;

$$\partial(n) = \partial(n-1) + k_{pifc}(I_{fc\_REF} - I_{fc}(n)) + k_{iifc}\sum_{k=0}^{n}(I_{fc\_REF} - I_{fc}(k)) \quad (1)$$

$$\partial(n) = \partial(n-1) + k_{pi}(I_{bat\_REF} - I_{bat}(n)) + k_{ii}\sum_{k=0}^{n}(I_{bat\_REF} - I_{bat}(k)) \quad (2)$$

$$\partial(n) = \partial(n-1) + k_{pv}(V_{bat\_REF} - V_{bat}(n)) + k_{iv}\sum_{k=0}^{n}(V_{bat\_REF} - V_{bat}(k)) \quad (3)$$

Where,

- I_{fc} is the sampled current from the fuel cell stack,
- V_{bat} the sampled voltage of the battery,
- I_{bat} the sampled current to the battery,
- $\partial(n)$ the duty cycles used to control the buck converter
- $\partial(n-1)$ the value of the duty cycle left off the last time when the particular mode was engaged,
- I_{fc_REF}, V_{bat_REF}, and I_{bat_REF} are the limits FCCL, BVL, and BCL, respectively,

k_{pifc},k_{iifc}, k_{pi}, k_{ii}, and k_{pv}, k_{iv} are the proportional and integral gains for the fuel cell current, battery current, and battery voltage, respectively.

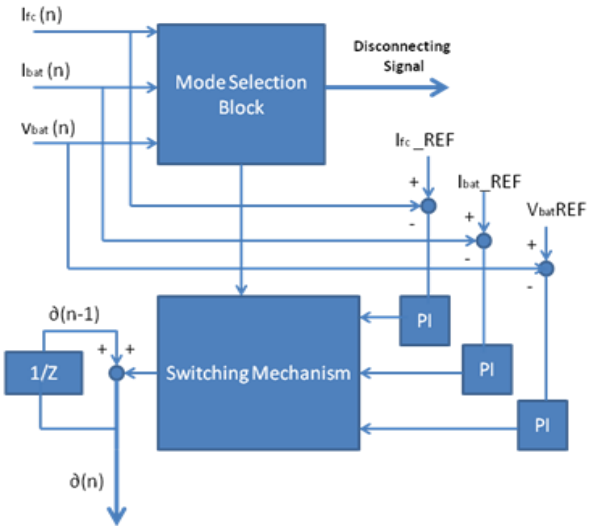

Fig. 6. Control Strstegy Block

C. Large-Signal Response

The control algorithm may force the system to frequently change from one operation mode to another due to load power demand and the battery charging. Hence there is a need to ensure large-signal stability of the system. The mode changes and the large signal behavior of the system are going to analyze here.

When the system operates at BCL mode, the rest of the system, seen by the battery, appears as a constant current source, and the battery charging current is regulated at the current limit, as illustrated in Fig. 7(a). In this mode, the operating point will move along the vertical line as the battery voltage increases, depending on the battery state of charge. The output power of the fuel cell depends on the load power requirement. When the system operates in BVL mode, the rest of the system, seen by the battery, appears as a constant voltage source, and the battery voltage is regulated at the voltage limit, as illustrated in Fig. 7(a). In this mode, the operating point will move along the horizontal line as the battery charging current decays. The output power of the fuel cell depends on the load power requirement.

When the load is increased such that the fuel cell current reaches the limit, the system will switch to FCCL mode. The output power of the fuel cell is constant since the current (or say, voltage) of the fuel cell is fixed by controlling the power converter. As mentioned before, if the load demand is low, the battery may be charged. Assuming that the load draws constant power within the time period we are interested in, the power transferred to the battery is constant, and the V –I curve of the battery is a constant power line, as shown in Fig. 7(b); thus, the battery current depends on the voltage. The battery power line will move leftward or rightward on the state plane when the load power changes (for instance, the dashed curve in Fig. 7(b) represents a different operating state than the continuous curve). If the load demand is so high that the battery discharges, the battery will provide an appropriate amount of current to compensate for the discrepancy between the fuel cell power and the load power, and the battery discharging current is unregulated. The increase in the load may cause the system to change from BCL mode to FCCL mode. The transition trajectory can be described by a line (line 1) on the state plane, the slope of which is equal to the equivalent series resistance of the battery in magnitude, as shown in Fig. 8(a). As a result of the mode transition, the battery charging current may decrease, and consequently, the battery terminal voltage decreases slightly. In the reverse, when the system changes from FCCL mode to BCL mode, the transition trajectory can be described by another line (line 2) on the state plane. As a result, the battery charging current increases and so does the battery terminal voltage. Both the voltage and the current of the battery will experience a sudden change when the system changes from BCL mode to FCCL mode or the reverse.

The increase in the load may also cause the system to change from BVL mode to FCCL mode. The transition trajectory can be described by line 3 on the state plane, the slope of which is also equal to the equivalent series resistance of the battery in magnitude, as shown in Fig. 8(b). As a result of the mode transition, the battery charging current may decrease, and consequently, the battery terminal voltage also decreases slightly. In the reverse, when the system changes from FCCL mode to BVL mode, the transition trajectory can be described by line 4 on the state plane. As a result, the battery charging current increases and so does the battery terminal voltage. Both the voltage and the current of the battery will experience sudden changes when the system changes from BVL mode to FCCL mode or the reverse. [17]

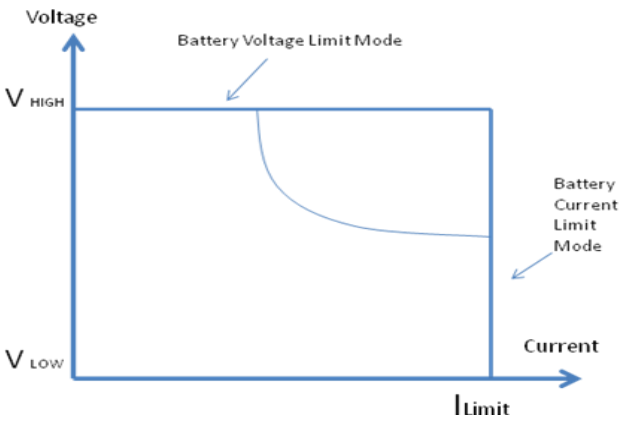

Fig. 7(a) V-I Characteristics Under Different Modes

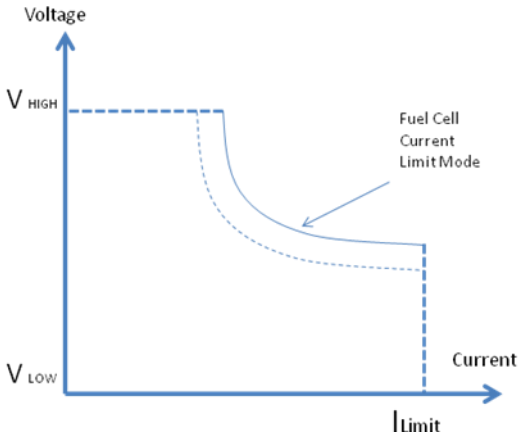

Fig. 7(b) V-I Characteristics Under Different Modes

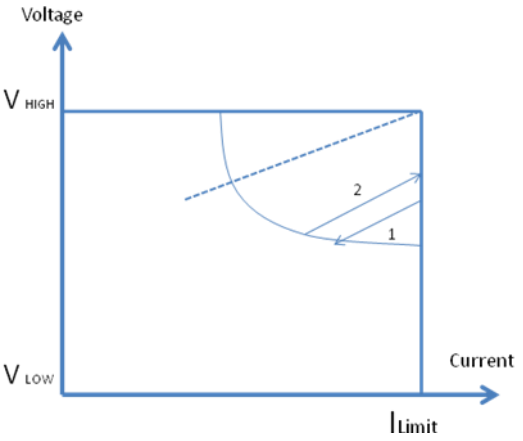

Fig. 8(a) V-I Characteristics from one Mode to another

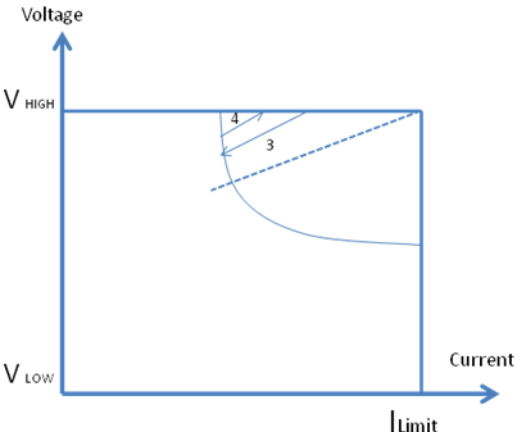

Fig. 8(b) V-I Characteristics from one Mode to another

IV. SIMULATIONS

A. *Simulink Model*

In order to test the suggested model and controller behavior, a MATLAB simulink based simulations were conducted. The simulink simulate the plant model including fuel cell stack, battery, H-Bridge and synchronous buck converter. Simulink will send the measured value of the current of fuel cell; battery and battery voltage to the MATLAB workspace, and then workspace interact with AVR via a serial connection. At each time step, the simulink simulates the plant model for one sample interval and export the system output to the microcontroller. The AVR receives signal from the simulink model, it executes the controller port and returns its computed control signal to the MATLAB via the same serial communication link.

Fig. 9 shows the simulink schematic view of the system model presented in the Fig. 2. The fuel cell stack model represents a 42-cell PEM fuel cell stack. The battery was configured as four cells in series and two strings in parallel. The nominal capacity of each cell was 1.6 Ah. The initial state-of-charge of the battery was 70%. A synchronous dc-dc buck converter represented the H-bridge based buck converter. The simout and simin block was an interface to the microcontroller, which was responsible for exchanging data between the simulation and the hardware. The load drew a pulse current of period of 10 s. The low current was 0.09 A for 9 s, and the high current was 6 A for 1 s. FCCL, BCL, and BVL were set as 3A, 2.5 A, and 18 V.

B. *Results*

Figs. 10–13 shows the simulations results. Battery and fuel cell voltages are shown in Fig. 10, when the battery voltage was far below the limit. Fig. 11 shows the currents of the fuel cell and the battery in this case. It is seen that when the load drew low power, the fuel cell stack provided current of about 2A, supplying 0.09A current to the load and charging the battery at 2.5A current at the same time. BCL mode applied and the battery charging current was regulated, at this time FCCL is not reached. The battery voltage was 17.4 V and the fuel cell voltage was around 22 V. FCCL mode is applied when the load drew peak power, and the fuel cell will supply its maximum of 3A current. In this case the battery discharged at approximately 4.2-A current. The fuel cell voltage dropped to 20.5V due to the higher current output, and the battery voltage dropped to 16.5V. It is seen that the currents of the fuel cell and the battery were regulated properly. It is also seen from the results that the fuel cell and battery currents experienced sudden changes as the mode changed between FCCL and BCL, as analyzed in the previous section. Fig. 12 shows the voltages of the fuel cell and the battery when the battery voltage approached the limit. Fig. 13 shows the currents of the fuel cell and the battery. The fuel cell stack provided about 2.2A current due to the load low power, supplying 0.09A current to the load and charging the battery at 2.5A current at the same time. In this case, the charging current of the battery was regulated (BCL mode applied), and the fuel cell current was less than the rated value (3A). After a while (at about 17 s), the battery voltage reached the voltage limit (18 V). The BVL mode then applied, and the battery voltage was regulated at a constant level (see Fig. 12). The battery charging current decreased slightly, and so did the fuel cell current. It is seen from the results that both the battery voltage and the battery current experienced continuous and gradual changes as the mode changed from BCL to BVL, as analyzed in the previous section. These results show that the simulation outputs matched

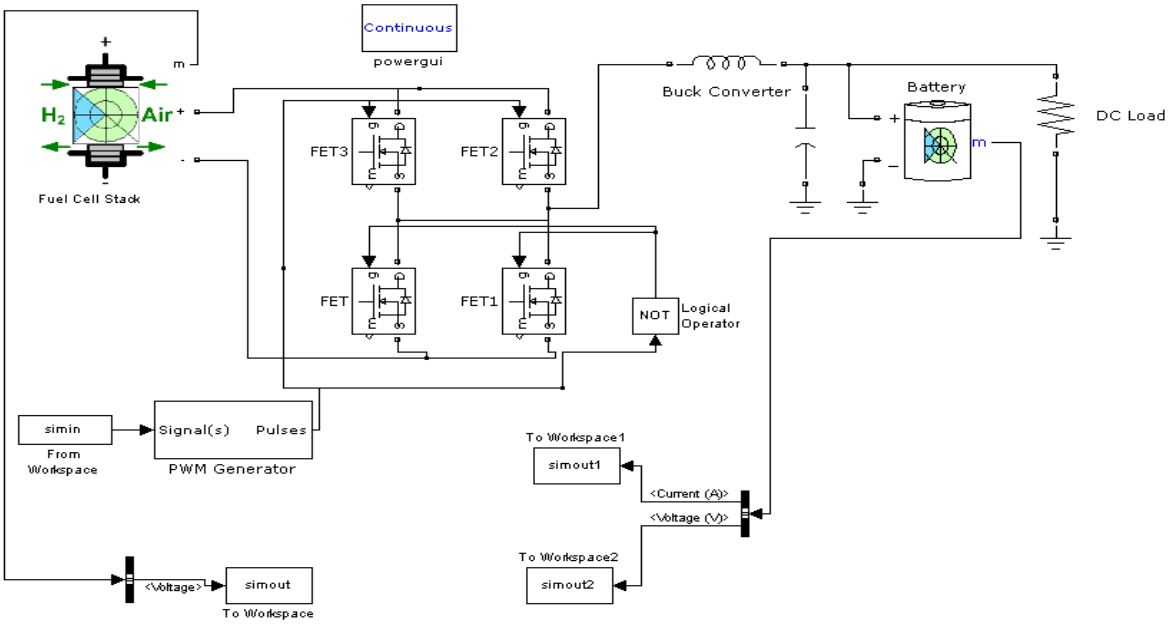

Fig. 9. Schematic diagram of simulink model

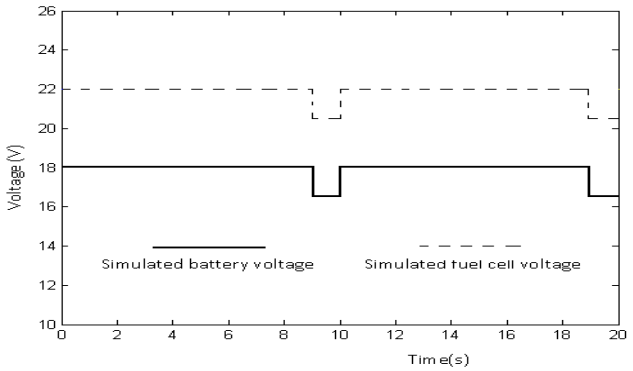

Fig. 10. Fuel Cell and Battery Voltage, when battery voltage was below the limit

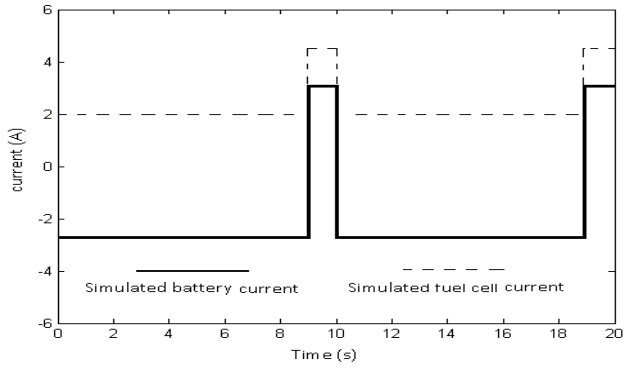

Fig. 11. Fuel Cell and Battery Current, when battery voltage was below the limit

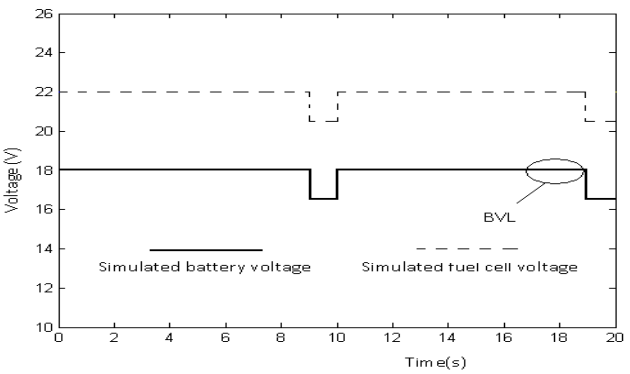

Fig. 12. Fuel Cell and Battery Voltage, when battery voltage approached the limit

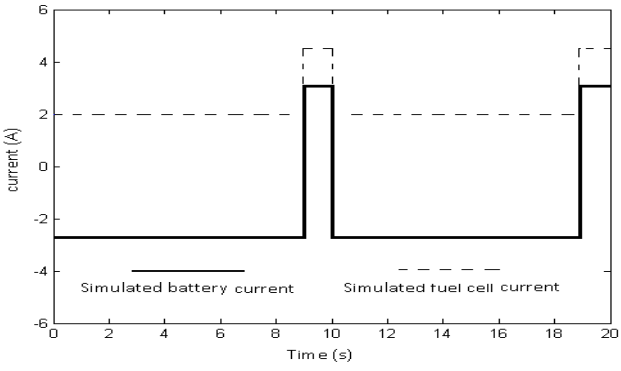

Fig. 13. Fuel Cell and Battery Current, when battery voltage approached the limit

the experimental data very well. It is also shown that the battery voltage and the currents of the fuel cell and the battery were regulated properly.

V. Conclusions

This paper has presented a compact embedded system controlled fuel cell/battery hybrid power source. Such a hybrid power source provides much higher peak power than each component alone while preserving high energy density, which is important and necessary to many modern electronic devices, through an appropriately controlled dc/dc power converter that handles the power flow shared by the fuel cell and the battery. Rather than being controlled to serve only as a voltage or current regulator, the power converter is regulated to balance the power flow to satisfy the load requirements while ensuring the various limitations of electrochemical components such as battery overcharge, FCCL, etc. Digital technology is applied in the control of the power converter due to many advantages over analog technology such as programmability, less susceptibility to environmental variations, and fewer part counts. The digital power controller circuit primarily consists of a synchronous buck converter that is controlled by an AVR microcontroller, with features of low power and higher efficiency. The user can set FCCL, BCL, and BVL in the digital controller. A control algorithm that is suitable for regulating the multiple variables in the hybrid system is described by using a state-machine-based model; the large-signal behavior of the hybrid system is analyzed on a voltage–current plane. The hybrid power source is then tested through simulation. Results show that the control algorithm is able to correctly select the regulation mode and appropriately limit the fuel cell current, the battery charging current, and the battery voltage.

References

[1] M. J. Blackwelder and R. A. Dougal, "Power coordination in a fuel cellbattery hybrid power source using commercial power controller circuits," J. Power Sources, vol. 134, no. 1, pp. 139–147, Jul. 2004.

[2] T. Chern, J. Chang, C. Chen, and H. Su, "Microprocessor-based modified discrete integral variable-structure control for UPS," IEEE Trans. Ind. Electron., vol. 46, no. 2, pp. 340–348, Apr. 1999.

[3] E. Koutroulis, K. Kalaitzakis, and N. C. Voulgaris, "Development of a microcontroller-based, photovoltaic maximum power point tracking control system," IEEE Trans. Power Electron., vol. 16, no. 1, pp. 46–54, Jan. 2001.

[4] A. S. Patil, T. G. Dubois, N. Sifer, E. Bostic, K. Gardner, M. Quah, and C. Bolton, "Portable fuel cell systems for America's army: Technology transition to the field," J. Power Sources, vol. 136, no. 2, pp. 220–225, Oct. 2004.

[5] K.Morita, "Automotive power source in 21st century," JSAE Rev., vol. 24, no. 1, pp. 3–7, Jan. 2003.

[6] L. Hedström, C. Wallmark, P. Alvfors, M. Rissanen, B. Stridh, and J. Ekman, "Description and modeling of the solar-hydrogen-biogasfuel cell system in GlashusEtt," J. Power Sources, vol. 131, no. 1/2, pp. 340–350, May 2004.

[7] T. Ruberti, "Off-grid hybrids: Fuel cell solar-PV hybrids," Refocus, vol. 4, no. 5, pp. 54–57, Oct. 2003.

[8] T. B. Atwater, P. J. Cygan, and F. C. Leung, "Man portable power needs of the 21st century: I. Applications for the dismounted soldier. II. Enhanced capabilities through the use of hybrid power sources," J. Power Sources, vol. 91, no. 1, pp. 27–36, Nov. 2000

[9] M. Nadal and F. Barbir, "Development of a hybrid fuel cell/battery powered electric vehicle," Int. J. Hydrogen Energy, vol. 21, no. 6, pp. 497–505, Jun. 1996

[10] R. F. Nelson, "Power requirements for batteries in hybrid electric vehicles," J. Power Sources, vol. 91, no. 1, pp. 2–26, Nov. 2000

[11] P. B. Jones, J. B. Lakeman, G. O. Mepsted, and J. M. Moore, "A hybrid power source for pulse power applications," J. Power Sources, vol. 80, no. 1/2, pp. 242–247, Jul. 1999.

[12] C. E. Holland, J.W.Weidner, R. A. Dougal, and R. E.White, "Experimental characterization of hybrid power systems under pulse current loads," J. Power Sources, vol. 109, no. 1, pp. 32–37, Jun. 2002.

[13] Z. Jiang, L. Gao, M. Blackwelder, and R. A. Dougal, "Design and experimental tests of control strategies for active hybrid fuel cell/battery power sources," J. Power Sources, vol. 130, no. 1, pp. 163–171, May 2004.

[14] L. Gao, Z. Jiang, and R. A. Dougal, "An actively controlled fuel cell/ battery hybrid to meet pulsed power demands," J. Power Sources, vol. 130, no. 2, pp. 202–207, May 2004.

[15] T. Kawabata, T. Miyashita, and Y. Yamamoto, "Digital control of three phase PWM inverter with LC filter," IEEE Trans. Power Electron., vol. 6, no. 1, pp. 62–72, Jan. 1991.

[16] S. Saggini, M. Ghioni, and A. Geraci, "An innovative digital control architecture for low-voltage, high-current DC-DC converters with tight voltage regulation," IEEE Trans. Power Electron., vol. 19, no. 1, pp. 210–218, Jan. 2004

[17] Z. Jiang and R. A. Dougal, "A compact digitally controlled fuel cell/battery hybrid power source," IEEE Trans. Ind. Electron., vol. 53, no. 4, pp. 1094–1104, Aug. 2006.